

# Growth of InAs Nanowires on SiO<sub>2</sub> Substrates: Nucleation, Evolution, and the Role of Au Nanoparticles

Shadi A. Dayeh, Edward T. Yu, and Deli Wang\*

Department of Electrical and Computer Engineering, Jacob's School of Engineering, University of California—San Diego, 9500 Gilman Drive, La Jolla, California 92093-0407

Received: May 3, 2007; In Final Form: July 6, 2007

We have studied the nucleation and growth of InAs nanowires (NWs) on SiO<sub>2</sub>/Si substrates by organometallic vapor-phase epitaxy (OMVPE). Through systematic characterization of InAs NW morphology as a function of V/III precursor ratio, precursor flow rates, growth temperature, growth time, and the presence/absence of Au nanoparticles, a number of significant insights into InAs NW growth using OMVPE have been developed. Specifically, we have found that (i) the growth of InAs NWs can be initiated from a single indium (In) droplet, (ii) Au nanoparticles (NPs) enhance group V precursor (AsH<sub>3</sub>) pyrolysis but are not necessary to nucleate growth, (iii) growth of InAs NWs on SiO<sub>2</sub> substrates occurs in the kinetically limited vapor–liquid–solid (VLS) growth regime, (iv) InAs NWs on SiO<sub>2</sub> films decompose at elevated temperatures even under significant AsH<sub>3</sub> overpressure, and (v) the V/III ratio is the growth-rate-limiting factor in the VLS growth of the InAs nanowires. Many of these findings on InAs NW growth can be generalized to and provide very useful information for rational synthesis of other III–V compound semiconductor NWs.

## Introduction

The growing interest in semiconductor nanowires (NWs) for electronic and photonic applications<sup>1–4</sup> necessitates rational control over their structure and key properties that requires thorough understanding of the growth mechanisms specific to the growth technique and material system. Metal-assisted NW growth for group IV, II–VI, and III–V semiconductor material systems was envisioned to occur via the vapor–liquid–solid (VLS) mechanism<sup>5</sup> for growth of Si whiskers, in which a liquid metal alloy (Au–Si) initiates the growth of a solid whisker (Si) from vapor reactants. However, there are some recent reports on different possibilities than the VLS growth, such as Ti-catalyzed growth of Si NWs in which the Ti seed particle is believed to remain in the solid phase during Si NW growth<sup>6</sup> in a process analogous to the VLS mechanism and the growth of GaAs NWs from Au nanoparticles where the Au nanocatalysts could possibly remain in the solid phase during NW growth, as indicated by transmission electron microscopy (TEM) analysis, at temperatures above those used for NW growth.<sup>7</sup> This growth mechanism was proposed to be the vapor–solid–solid (VSS) growth mechanism, which relies on the solid-phase diffusion of a single component (group III) through a solid seed particle. The observation of cessation of InAs NW growth at temperatures higher than the “melting temperature” of Au–In alloy was taken to be further evidence for the VSS growth mechanism.<sup>8</sup>

Although NW growth is often initiated by Au nanoparticle catalysts, NW growth in the absence of a “foreign” metal catalyst has been reported using various growth techniques such as (1) the growth of GaAs and AlGaAs NWs on GaAs(111)B substrates using selective-area metal organic vapor-phase epitaxy (SA-MOVPE),<sup>9</sup> (2) epitaxial growth of In-catalyzed InP NWs on InP(111)B substrates,<sup>10</sup> (3) oxide-assisted growth of GaAs NWs on Si substrates through laser ablation of a mixture of

GaAs and GaO<sub>3</sub>,<sup>11</sup> and (4) Au-free epitaxial growth of InAs NWs on InP(111)B and InAs(001) substrates.<sup>12</sup> These examples of the growth of NWs in the absence of the metal particle raise the question of the particle's role in metal-assisted NW growth.

In this paper, we report studies of nucleation and growth of InAs NWs on SiO<sub>2</sub>/Si substrates in an organometallic vapor-phase epitaxy (OMVPE) reactor and systematic characterization of InAs NW morphology as a function of V/III precursor ratio, precursor flow rates, substrate growth temperature, growth time, and the presence or absence of Au nanoparticles. Our results indicate that In droplets act as seeds for InAs NW growth while the Au nanoparticles catalyze the pyrolysis of AsH<sub>3</sub> precursor, and the V/III ratio is a limiting factor in the growth rate of the InAs NWs.

## Experimental Section

The InAs NW growth was performed in a horizontal OMVPE reactor at a pressure of 100 torr with trimethylindium (TMIn) and arsine (AsH<sub>3</sub>) precursors in 1.2 slm (standard liters per minute) of H<sub>2</sub> carrier gas. Growth was conducted over a substrate temperature range of 300–390 °C on Si substrates with 600 nm thermally grown oxide. The 40 nm diameter Au nanoparticles from colloidal solution were dispersed on the substrate surface prior to growth at an average particle density of 0.21 particles/μm<sup>2</sup>. For all growth experiments, the temperature was ramped up at a rate of ~2 °C/s and allowed to stabilize at the growth temperature in H<sub>2</sub> ambient. The reaction precursors were introduced for the duration of the growth run, after which AsH<sub>3</sub> flow was maintained during the cool down for 2 min followed by a 2 min H<sub>2</sub> purge; the reactor was then left in N<sub>2</sub> ambient until sample removal. The input V/III precursor ratio was varied between ~30–90 by adjusting the AsH<sub>3</sub> flow rate (44–134 μmol/min) and maintaining a constant TMIn flow rate of 1.5 μmol/min. The growth times were varied in the range of 30–600 s. The morphology of nanoparticles and NWs was characterized using an FEI XL 30 environmental scanning

\* Corresponding author. Tel.: (+1) 858-822-4723. Fax: (+1) 858-534-0556. E-mail: dwang@ece.ucsd.edu.

electron microscope (ESEM) operating at 10 kV acceleration voltage. Dimensions and statistical distributions of nanoparticles, islands, and InAs NWs were determined in each case by measuring the sizes of 50 particles or wires at  $\sim 600\,000\times$  magnification.

## Results and Discussion

The catalytic effect of Au nanoparticles in NW nucleation and growth is of critical importance to the understanding of their growth mechanism and has been the subject of extensive recent studies.<sup>5–12</sup> However, the significant catalytic effect of Au nanoparticles to precursor pyrolysis in NW growth received less attention. Specifically, it is known that Au has the ability to form the weakest bonds and hence has the highest surface reactivity among all metals.<sup>13</sup> Therefore, the pyrolysis temperatures of the precursors are expected to be lower when Au is present in the chamber. In order to study the catalytic effect of Au nanoparticles on precursor pyrolysis, we have investigated the nucleation of InAs NWs on  $\text{SiO}_2/\text{Si}$  substrates (i.e., a nonreactive substrate) in the presence or absence of Au nanoparticles at different growth temperatures. Figure 1A shows a schematic of the experiment design with varying growth temperature, precursors input sequence, and the presence or absence of the Au nanoparticles indicated for each experiment (I–VIII).

In experiment I, 40 nm diameter Au nanoparticles were dispersed on the  $\text{SiO}_2/\text{Si}$  substrate at a particle density of  $\sim 10$  particles/ $\mu\text{m}^2$  and TMIn flow ( $6\ \mu\text{mol}/\text{min}$ ) was introduced for 6 min at  $350\ ^\circ\text{C}$ . The diameter of the nanoparticles increased to  $\sim 50$ – $200$  nm, and a spherical shape is maintained due to Au–In alloying, as shown in Figure 1B (a higher magnification image is shown in the Supporting Information Figure 1S). This occurs because at  $350\ ^\circ\text{C}$  and in  $\text{H}_2$  ambient, TMIn pyrolysis is complete on  $\text{SiO}_2$  surfaces.<sup>14</sup> This substrate with Au–In alloy nanoparticles from experiment I was then cleaved outside the growth tube into two pieces for experiments II and III. In experiment II, the sample was subjected to an  $\text{AsH}_3$  flow of  $74\ \mu\text{mol}/\text{min}$  for 6 min at  $350\ ^\circ\text{C}$ . The spherical Au–In nanoparticles crystallize and form InAs islands as shown in the SEM micrograph in Figure 1C and confirmed by energy dispersive X-ray (EDX) analysis (see the Supporting Information Figure 2S for EDX spectra) but with no NW growth. Because  $\text{AsH}_3$  is only 50% pyrolyzed even at  $600\ ^\circ\text{C}$  on  $\text{SiO}_2$  surfaces in  $\text{H}_2$  ambient and in the absence of TMIn and Au nanoparticles,<sup>15</sup> the partly pyrolyzed  $\text{AsH}_3$  and the already deposited In were insufficient to create the concentration gradient required to initiate InAs NW growth.<sup>16</sup> To further investigate this point, we performed experiment III, where the sample was subjected to TMIn and  $\text{AsH}_3$  flows of 6 and  $74\ \mu\text{mol}/\text{min}$ , respectively, at  $350\ ^\circ\text{C}$  for the same growth time (6 min) resulting in significant NW growth on the substrate as shown in Figure 1D. Similar results to those of experiments II and III were obtained without interrupting the growth run for sample cleavage. From experiments II and III, we conclude that NW growth was only possible when TMIn and  $\text{AsH}_3$  are present in the chamber simultaneously even in the presence of Au–In alloy on the  $\text{SiO}_2$  substrate; from this, we deduce that the presence of TMIn plays an important role in  $\text{AsH}_3$  pyrolysis and thus NW growth. When both TMIn and  $\text{AsH}_3$  are present in the reaction chamber, the pyrolysis temperatures are expected to be reduced significantly with heterogeneous reactions dominating the precursor pyrolysis at low temperatures.<sup>17</sup> Studies on  $\text{AsH}_3$  pyrolysis in the presence of TMGa have shown that the  $\text{AsH}_3$  pyrolysis temperatures are reduced by  $\sim 200\ ^\circ\text{C}$ .<sup>18</sup>

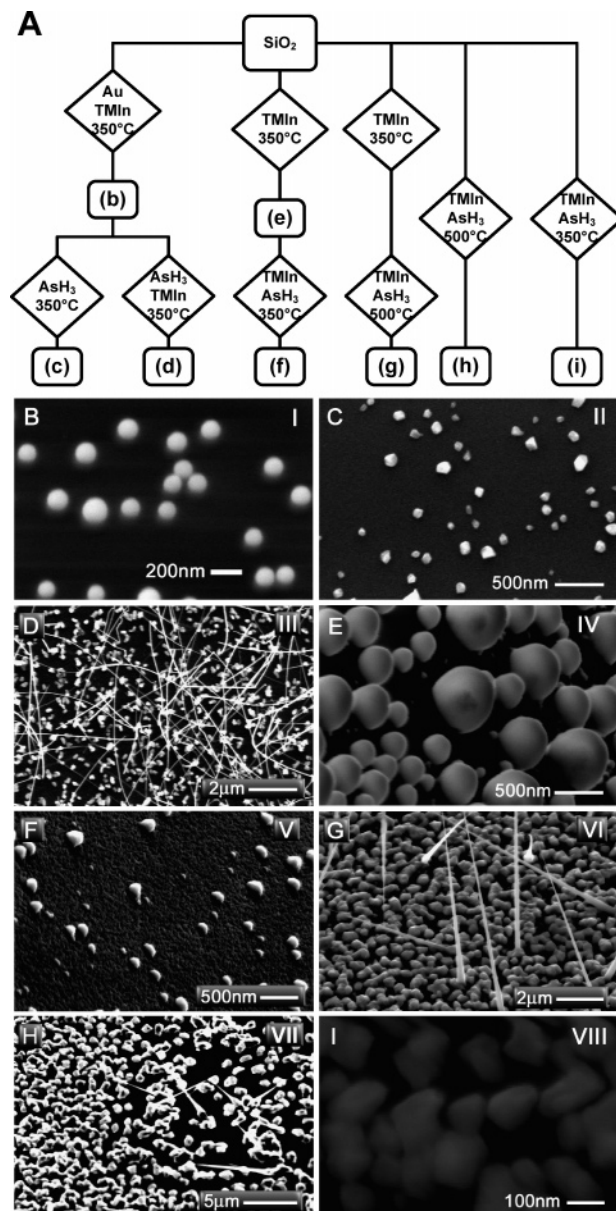


**Figure 1.** (A) Schematic diagram showing MOCVD growth experiment details on the  $\text{SiO}_2$  substrate. (B–D) SEM images of (B) In–Au nanoparticles after TMIn exposure; (C) half of the sample in (B) after  $\text{AsH}_3$  exposure; (D) half of the sample in (B) after  $\text{AsH}_3$  and TMIn exposure. (E–I) In the absence of Au nanoparticles, SEM images of (E) In droplets formed after TMIn exposure; (F) the sample in (E) after TMIn and  $\text{AsH}_3$  exposure; (G) same as in (E) at a growth temperature of  $500\ ^\circ\text{C}$ ; (H) InAs NWs grown on the  $\text{SiO}_2$  surface after TMIn and  $\text{AsH}_3$  flow at  $500\ ^\circ\text{C}$ ; (I) InAs islands formed on the  $\text{SiO}_2$  surface after TMIn and  $\text{AsH}_3$  flow at  $350\ ^\circ\text{C}$  with no NW growth.

As a comparison study, a second set of experiments was carried out on  $\text{SiO}_2$  substrates without Au nanoparticles on top. In experiment IV, a bare  $\text{SiO}_2$  substrate is exposed to  $6\ \mu\text{mol}/\text{min}$  of TMIn at  $350\ ^\circ\text{C}$  for 6 min resulting in sufficient TMIn pyrolysis for formation of In droplets, as shown in Figure 1E. This sample was then used in experiment V for comparison to experiment III, where the substrate was subjected to identical growth conditions, i.e., flow of 6 and  $74\ \mu\text{mol}/\text{min}$  of TMIn and  $\text{AsH}_3$ , respectively, at  $350\ ^\circ\text{C}$  for 6 min. No NW growth was observed from experiment V, as shown in Figure 1F, indicating that the presence of the Au nanoparticles on the substrate is essential for efficient  $\text{AsH}_3$  pyrolysis at  $350\ ^\circ\text{C}$ . However, in experiment VI with the same growth time and flow rates as in experiment V but a substrate temperature of  $500\ ^\circ\text{C}$ ,

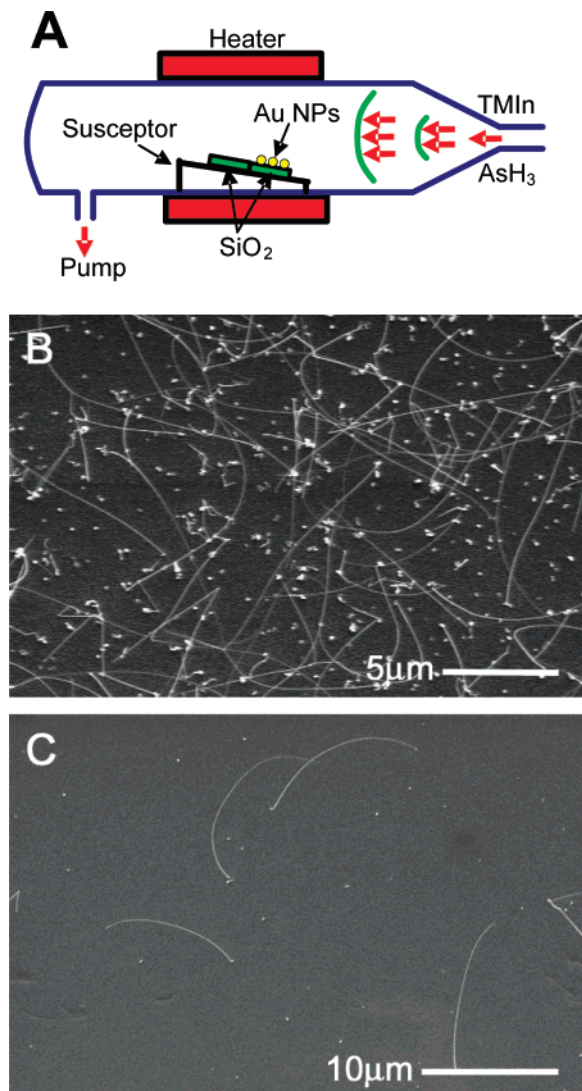


**Figure 2.** (A) Schematic diagram showing the growth setup for the remote effect of the Au nanoparticles in the AsH<sub>3</sub> pyrolysis on SiO<sub>2</sub> substrate. (B) SEM image of NWs grown on the upstream SiO<sub>2</sub> sample with Au nanoparticles on top. (C) SEM image of NWs grown on the downstream SiO<sub>2</sub> sample with no Au nanoparticles on top.

NW growth was observed on the bare SiO<sub>2</sub> substrate due to improved AsH<sub>3</sub> pyrolysis at 500 °C as shown in Figure 1G. Furthermore, the predeposition step of In droplets at 350 °C is not necessary because the TMIn pyrolysis is efficient at 500 °C. Indeed, experiment VII demonstrates NW growth on the bare SiO<sub>2</sub> surface at 500 °C, as shown in Figure 1H. Finally, no NW growth at 350 °C was observed on the bare SiO<sub>2</sub>/Si substrate from experiment VIII with identical TMIn and AsH<sub>3</sub> flows as in I–VII, as shown in Figure 1I. Thus, we conclude that AsH<sub>3</sub> pyrolysis is a limiting factor in the InAs NW growth, and our results suggest that Au nanoparticles help in the AsH<sub>3</sub> pyrolysis process.

To further assess the role of the Au nanoparticles, we loaded a bare SiO<sub>2</sub>/Si sample with no Au nanoparticles on top downstream from another SiO<sub>2</sub> substrate onto which Au nanoparticles had been dispersed, as shown schematically in Figure 2A. NW growth at 350 °C was observed not only on the SiO<sub>2</sub> substrate with Au nanoparticles on top, as shown in Figure 2B, but also on the bare SiO<sub>2</sub> substrate that was not dispersed with Au catalysts, as shown in Figure 2C; the growth on the bare SiO<sub>2</sub> substrate is different from the growth of experiment VIII shown in Figure 1I, where only InAs islands

form on a bare SiO<sub>2</sub> substrate under the same growth conditions. The NWs grown on the SiO<sub>2</sub> substrate with Au nanoparticles are long, bent, and tapered. There is a very large diameter variation, and the diameter does not appear to be defined by the initial Au nanoparticle size as normally seen in Au nanoparticle-mediated VLS NW growth. There are InAs islands (solidified from Au–In alloy particles) that are much larger in size (50–300 nm) after NW growth, some of which grow multiple NWs. Typically, no “catalyst” was found at the tip of the NWs under SEM. The InAs NWs grown on the bare SiO<sub>2</sub> substrate have very similar morphologies, but the InAs islands on the substrate are smaller. NW growth on the bare SiO<sub>2</sub> substrate was also reproduced at a 0.4 mm separation from the SiO<sub>2</sub> substrate with Au nanoparticles on top. Similar experiments were also carried out on patterned substrates, with growth conducted under identical conditions on SiO<sub>2</sub> substrates with a 10 nm Au thin film deposited at the center of the substrate using a shadow mask. No InAs NW growth was observed upstream from the Au film, but there is NW growth downstream from the Au film area at a separation distance of ≥1.5 mm. There is no NW growth for distances <1.5 mm, presumably due to the depletion of In necessary for the NW growth sites at the peripheries of the Au film. Moreover, there is no NW growth gradient observed downstream from the Au film. These experiments exclude the possibility in our studies of transport of the metal catalyst via droplet breakup during the growth, as reported recently for Si NW growth.<sup>19</sup> Moreover, InAs NW growth was observed only at the peripheries of the Au film and not at its center due to the higher local V/III ratio at the center of the sample that inhibits NW growth, which we will discuss later in this article.

These experiments demonstrate that at temperatures around 350 °C, the Au nanoparticles play an important role in catalyzing the AsH<sub>3</sub> pyrolysis. Specifically, the observations that Au–In forms much larger particle sizes from which multiple NWs grow from a single island and the NW growth on bare SiO<sub>2</sub> substrate without Au nanoparticles indicate that the presence of Au nanoparticles is important for reactant pyrolysis at moderate growth temperatures but the nanoparticles do not necessarily directly nucleate NW growth. This catalytic effect has also been observed in other III–V NW growth; for example, study of the growth of GaP NWs has shown that the dissociation reaction of PH<sub>x</sub> on the catalytic Au surface is the rate-limiting step for the growth of GaP NWs.<sup>20</sup> The possible origin for the one-dimensional (1D) NW growth we observe at this temperature is a liquid group III (In) droplet (or In-rich Au–In alloy) that serves as a catalyst for VLS NW growth. Indeed, it had been suggested by Wagner and Ellis that the metal “impurity” in VLS growth could be an excess of one of the material constituents for growth of compound semiconductor NWs.<sup>5</sup> An atomic probe microscopy experiment could help to analyze the incorporation of Au elements in InAs NWs and further illustrate involvement of Au in the InAs NW growth.<sup>21</sup> The postgrowth absence of an alloy droplet on the NW tips for longer growth runs, and within the resolution limits of the SEM imaging (see the Supporting Information Figure 3S for SEM images of the NW tip), can be attributed to In consumption during temperature cooling down in AsH<sub>3</sub> flow after NW growth. Although very unlikely, In evaporation during growth, as seen in Ga evaporation from Ga droplets in the GaAs whisker growths, cannot be ruled out.<sup>22</sup>

To further investigate the nucleation and evolution of InAs NWs during growth, we monitored the morphological changes of the Au nanoparticles by SEM imaging for different growth times but otherwise identical growth conditions (with an input

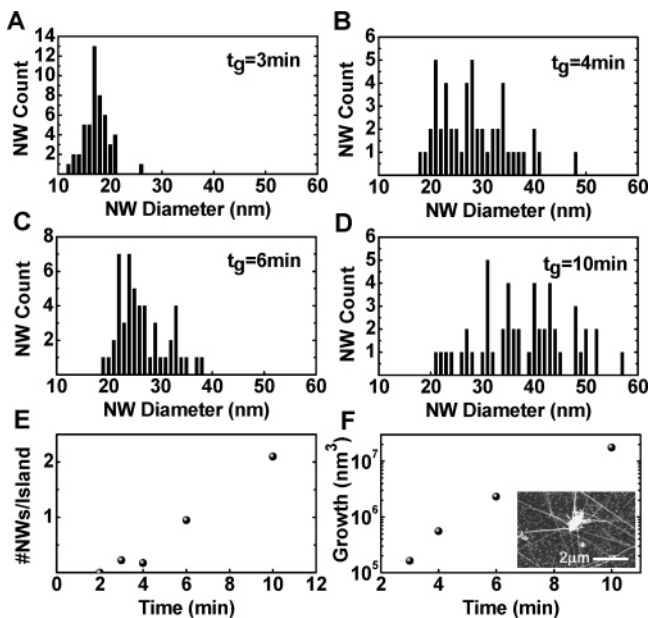


**Figure 3.** (A–D) Histograms of NW diameter variation for different growth times. (E) Number of InAs NWs per single island for different growth times. (F) Total NW growth as function of growth time. Inset is an SEM image of a single InAs island from which several NWs have nucleated.

V/III ratio of 25 and growth temperature of 350 °C). After short growth intervals (30–90 s), the apparent Au colloid diameter increased to ~55 from 40 nm due to InAs deposition on the Au colloid, but spherical shape is maintained. For longer growth runs up to 3 min, InAs islands with irregular shapes were observed to form on the substrate with density comparable to that of the deposited Au nanoparticles, suggesting that one island forms around each Au nanoparticle, but there is no NW formation. NWs were observed to nucleate and grow for growth times longer than 3 min. Figure 3A–D shows histograms of NW diameter distribution for different growth times. It is evident that the NWs start to grow with very thin diameters, mostly smaller than that of the 40 nm Au nanoparticles. A very large variation in NW diameter is observed with the average NW diameter and dispersity increasing with growth time: the NWs have diameters ranging from 12 to 26 nm, 18 to 47 nm, and 20 to 57 nm for growth times of 3, 4, and 10 min, respectively. NW length increases with growth time as well, ranging from 0.3 to 17  $\mu\text{m}$  for growth times from 3 to 10 min. The increases in NWs diameter and length indicate VLS growth in the axial direction and VS growth in the radial direction. For longer growth runs, multiple NWs were observed to grow from single InAs islands, as shown in the SEM image in the inset of Figure 3F. The number of NWs grown per island increases with time, as shown in Figure 3E (see the Supporting Information Figure 4S). These results suggest a growth mechanism different from the Au-mediated VLS or VSS growth, and provide further evidence that Au nanoparticles are not necessarily initiating NW growth, and that NW growth is nucleated by In droplets in our study.

Due to the NW diameter variation for different growth times, growth rate is calculated in terms of the average NW volume instead of length. Furthermore, because there is more than one NW per single InAs island, we can further normalize the growth rate with respect to the number of islands and calculate the NW growth as function of time using

$$\rho = \frac{\sum_{i=1}^N \pi d_i^2 L_i}{N t} M \quad (1)$$

where  $\rho$  is the NW growth rate,  $d$  and  $L$  are the NW diameter and length, respectively,  $N = 50$  is the number of characterized NWs,  $M$  is the number of NWs per single InAs island, and  $t$  is the growth time. The resulting growth rate is plotted in Figure 3F. The island volume change is negligible compared to the NW volume change with time and, thus, was not included in calculating the growth rate. Note that the NW length increases steadily with increasing growth time, with no restriction imposed by the diffusion length of any of the reactants on the  $\text{SiO}_2$  substrate or the InAs NW. This is highly plausible due to the high mobility of In on the  $\text{SiO}_2$ , as observed for NW growth using SA-OMVPE.<sup>9</sup>

To assess the influence of substrate temperature, InAs NW growth was studied at temperatures ranging from 310 to 390 °C for 6 min with fixed TMI and  $\text{AsH}_3$  flows. At 310 °C, there is no NW growth due to inefficient pyrolysis of the input precursors. NWs start to grow at temperatures higher than 330 °C, and the growth rate (volume/time) increases exponentially with substrate temperature as shown in Figure 4, indicating kinetically limited NW growth with activation energy of ~56 kcal/mol. The NWs are tapered, but SEM imaging indicates the tapering is minimal for NW growth at temperatures up to 350 °C (approximately 1.37 nm/ $\mu\text{m}$  measured from tip to root). The tapering becomes more severe at higher temperatures, due to the enhanced sidewall coating because of the excess material supplied and increased VS growth.

The InAs NWs grown on  $\text{SiO}_2$  substrates suffer severe morphological changes at higher temperatures even under  $\text{AsH}_3$  flow. Significant morphological change of NWs grown at 350 °C and a sharp decrease in the NW density were observed when the substrate was heated up to 450 °C in 444  $\mu\text{mol}/\text{min}$   $\text{AsH}_3$  flow. This indicates severe As outgassing and decomposition of the InAs NWs at 450 °C due to insufficient  $\text{AsH}_3$  pyrolysis. At 500 °C, but with both TMI and  $\text{AsH}_3$  flows into the reactor, only morphological imperfections with no drop in the NW density were observed, which can be attributed to the enhanced As pyrolysis due to the simultaneous presence of TMI and  $\text{AsH}_3$ . These experiments confirm the importance of maintaining  $\text{AsH}_3$  flow during cool down after NW synthesis, similar to the growth of two-dimensional (2D) epilayers.

The input V/III ratio also emerges in our studies as an important limiting factor for compound semiconductor NW growth. The  $\text{SiO}_2$  surface provides a unique platform for studying InAs NW growth as a function of V/III ratio because there is no local altering of input V/III ratio from the  $\text{SiO}_2$  substrate surface, in contrast to the involvement of substrate decomposition for growth on InAs substrates.<sup>23</sup> A set of growth experiments was conducted at 350 °C for 6 min at different V/III ratios; a growth temperature of 350 °C was chosen because minimal tapering was observed in our earlier studies at this temperature. By varying the  $\text{AsH}_3$  flow rate over a range of 44–134  $\mu\text{mol}/\text{min}$  and maintaining a constant TMI flow rate at ~1.5  $\mu\text{mol}/\text{min}$ , the input V/III ratio was varied between 30 and 90. The InAs NW diameters, lengths, and density decrease as the input V/III ratio increases, as shown by the NW volume growth rate versus V/III ratio plot in Figure 5A. At constant TMI flow, growth pressure, and temperature on a  $\text{SiO}_2/\text{Si}$  substrate, the input V/III ratio determines the growth rate, and the partial pressures at the growth interface (and consequently,

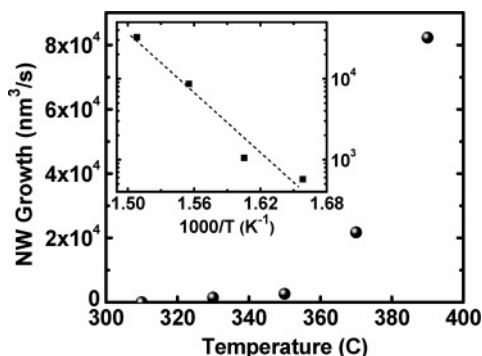


**Figure 4.** NW growth rate as function of growth temperature on the SiO<sub>2</sub> surface. Inset is an Arrhenius plot of the growth rate.

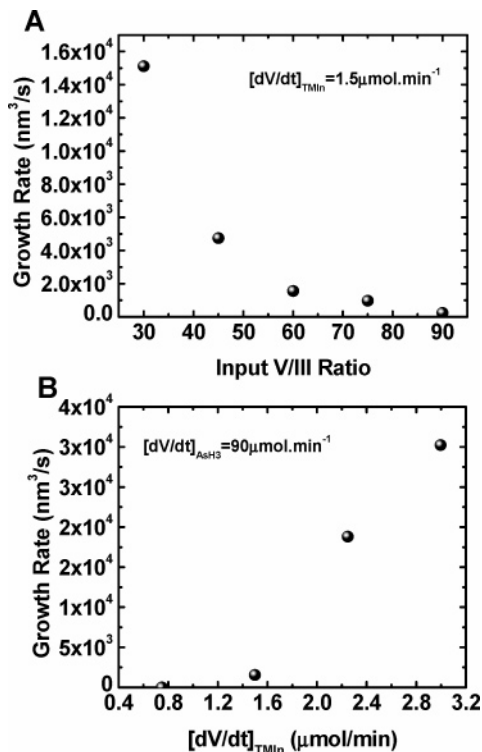


**Figure 5.** (A) NW growth rate as function of the input V/III ratio with constant TMIn flow rate. (B) NW growth rate as function of TMIn flow rate with the AsH<sub>3</sub> flow rate maintained constant.

the interface V/III ratio) determine the solid stoichiometry.<sup>17</sup> The activation energies for heterogeneous reactions tend to decrease with increasing V/III ratio in thin film deposition,<sup>24</sup> and as a result the thin film growth rate increases with increasing V/III ratio. On the other hand, InAs crystallization may consume the available In required for NW nucleation and hinder its supply to the seed particle,<sup>25</sup> leading to a decrease in the NW growth rate with increasing V/III ratio. We also observed in these experiments that InAs island deposition on the SiO<sub>2</sub> surface increases as the input V/III ratio increases. This also explains our observation of InAs NW growth only at the peripheries of the Au film but not at its center: There exists a very high local V/III ratio at the center of the Au film due to enhanced AsH<sub>3</sub> pyrolysis leading to suppression of NW growth in this area. We have also performed InAs NW growth at different V/III ratios with fixed AsH<sub>3</sub> flow (~90 μmol/min) and varying TMIn flow rate (~0.75–3 μmol/min). Figure 5B shows a plot of the NW growth rate as function of the TMIn flow rate, revealing that the growth rate increases with increasing TMIn flow. This

trend is similar to thin film epitaxy whose growth rate is known to be determined by the group III flow rate. For the InAs NW growth rate in Figure 5B, the V/III ratio decreases with increasing TMIn flow leading to an enhancement in the NW growth rate.

## Conclusion

In conclusion, we have studied the nucleation and growth evolution of InAs NWs on SiO<sub>2</sub>/Si substrates. By varying key growth parameters such as presence or absence of Au nanoparticles, sequential input and flow rates of TMIn and AsH<sub>3</sub> precursors, growth time, substrate temperature, and input V/III ratio, significant insights into the InAs NW growth have been developed. The Au nanoparticles were found to facilitate efficient pyrolysis of AsH<sub>3</sub> but are not necessary to nucleate InAs NW growth. InAs NWs are most likely nucleated through In seed particles created from excess In supply on the substrate, and grow via the VLS growth mechanism; this conclusion is also supported by the observation of InAs NW growth using a simple closed CVD system.<sup>26</sup> The input V/III ratio was shown to play a critical role in NW growth. These findings are very useful for understanding and rational synthesis of InAs and other III–V compound semiconductor NWs.

**Acknowledgment.** We acknowledge the financial support of the Office of Naval Research (ONR-nanoelectronics), National Science Foundation (ECS-0506902), and Sharp Labs of America. S. A. Dayeh is also grateful for the W.S.C. Chang's fellowship support during the period of this study, to Clint Novotny for OMVPE operation training, and David P. R. Aplin for discussion.

**Supporting Information Available:** Cross-sectional FE-SEM of a Au–In droplet showing spherical curvature, EDX spectra of InAs islands, close-up SEM to the InAs NW tip showing no Au particle at the tip for NWs grown on SiO<sub>2</sub> and a Au particle at the tip of NW grown on InAs(111)B, FE-SEM images of NWs grown for different times showing evolution of multiple NW growth per single InAs island for longer growth times. This material is available free of charge via the Internet at <http://pubs.acs.org>.

## References and Notes

- (1) Lieber, C. M.; Wang, Z. L. *MRS Bull.* **2007**, *32*, 99.
- (2) Li, Y.; Qian, F.; Xiang, J.; Lieber, C. M. *Mater. Today* **2006**, *9*, 18.
- (3) Thelander, C.; Agarwal, P.; Brongersma, S.; Eymery, J.; Feiner, L. F.; Forchel, A.; Scheffler, M.; Riess, W.; Ohlsson, B. J.; Gösele, U.; Samuelson, L. *Mater. Today* **2006**, *9*, 28.
- (4) Pauzaskie, P. J.; Yang, P. *Mater. Today* **2006**, *9*, 36.
- (5) Wagner, R. S.; Ellis, W. C. *Appl. Phys. Lett.* **1964**, *4*, 89.
- (6) Kamins, T. I.; Williams, R. S.; Basile, D. P.; Hesjedal, T.; Harris, J. S. *J. Appl. Phys.* **2001**, *89*, 1008.
- (7) Persson, A. I.; Larsson, M. W.; Stenström, S.; Ohlsson, B. J.; Samuelson, L.; Wallenberg, L. R. *Nat. Mater.* **2004**, *3*, 677.
- (8) Dick, K. A.; Deppert, K.; Martensson, T.; Mandl, B.; Samuelson, L.; Seifert, W. *Nano Lett.* **2005**, *5*, 761.
- (9) Motohisa, J.; Takeda, J.; Inari, M.; Noborisaka, J.; Fukui, T. *Physica E* **2004**, *23*, 298.
- (10) Novotny, C. J.; Yu, P. K. L. *Appl. Phys. Lett.* **2005**, *87*, 203111.
- (11) Shi, W. S.; Zheng, Y. F.; Wang, N.; Lee, C. S.; Lee, S. T. *Appl. Phys. Lett.* **2001**, *78*, 3304.
- (12) Mandl, B.; Stang, J.; Martensson, T.; Mikkelsen, A.; Eriksson, J.; Karlsson, L. S.; Bauer, G.; Samuelson, L.; Seifert, W. *Nano Lett.* **2006**, *6*, 1817.
- (13) Hammer, B.; Nørskov, J. K. *Nature* **1995**, *376*, 238.
- (14) Buchan, N. I.; Larsen, C. A.; Stringfellow, G. B. *J. Cryst. Growth* **1988**, *92*, 591.

- (15) Larsen, C. A.; Buchan, N. I.; Stringfellow, G. B. *Appl. Phys. Lett.* **1988**, *52*, 480.
- (16) Wagner, R. S. In *Whisker Technology*; Levitt, A. P., Ed.; Wiley-Interscience: New York, 1970.
- (17) Stringfellow, G. B. *Organometallic Vapor-Phase Epitaxy, Theory and Practice*; Academic Press, 1999.
- (18) Larsen, C. A.; Li, S. H.; Stringfellow, G. B. *Chem. Mater.* **1991**, *3*, 39.
- (19) Cao, L.; Garipcan, B.; Atchison, J. S.; Ni, C.; Nabet, B.; Spanier, J. E. *Nano Lett.* **2006**, *6*, 1852.
- (20) Verheijen, M. A.; Immink, G.; de Smet, T.; Borgström, M. T.; Bakkers, P. A. M. E. *J. Am. Chem. Soc.* **2005**, *128*, 1353.
- (21) Perea, D. E.; Allen, J. E.; May, S. J.; Wessels, B. W.; Seidman, D. N.; Lauhon, L. J. *Nano Lett.* **2005**, *6*, 181.
- (22) Givargizov, E. I. *Highly Anisotropic Crystals*; Terra Scientific Publishing Company, 1987.
- (23) Dayeh, S. A.; Yu, E. T.; Wang, D. *Nano Lett.*, submitted for publication, 2007.
- (24) Reep, D. J.; Ghandi, S. K. *J. Electrochem. Soc.* **1984**, *131*, 2697.
- (25) Kasahara, J.; Kajiwara, K.; Yamada, T. *J. Cryst. Growth* **1977**, *38*, 23.
- (26) Park, H. D.; Prokes, S. M.; Cammarata, R. C. *Appl. Phys. Lett.* **2005**, *87*, 063110.